Poly(ethylene oxide) Layers Grafted to Dopamine-melanin Anchoring Layer: Stability and Resistance to Protein Adsorption

6 AUTHORS, INCLUDING:

Ognen Pop-Georgievski
Academy of Sciences of the Czech Republic
23 PUBLICATIONS 240 CITATIONS

SEE PROFILE

Vladimir Proks
Academy of Sciences of the Czech Republic
37 PUBLICATIONS 291 CITATIONS

SEE PROFILE

Frantisek Rypacek
Academy of Sciences of the Czech Republic
94 PUBLICATIONS 938 CITATIONS

SEE PROFILE

Poly(ethylene oxide) Layers Grafted to Dopamine-melanin Anchoring Layer: Stability and Resistance to Protein Adsorption

Ognen Pop-Georgievski,*,[†] Štěpán Popelka,[†] Milan Houska,[†] Dagmar Chvostová,[‡] Vladimír Proks,[†] and František Rypáček[†]

[†]Institute of Macromolecular Chemistry, Academy of Sciences of the Czech Republic, Heyrovsky sq. 2, 162 06 Prague 6, Czech Republic

[‡]Institute of Physics, Academy of Sciences of the Czech Republic, Na Slovance 2, 182 21 Prague, Czech Republic

S *Supporting Information*

ABSTRACT: In this study, we propose substrate-independent modification for creating a protein-repellent surface based on dopamine-melanin anchoring layer used for subsequent binding of poly(ethylene oxide) (PEO) from melt. We verified that the dopamine-melanin layer can be formed on literally any substrate and could serve as the anchoring layer for subsequent grafting of PEO chains. Grafting of PEO from melt in a temperature range 70—110 °C produces densely packed PEO layers showing exceptionally low protein adsorption when exposed to the whole blood serum or plasma. The PEO layers prepared from melt at 110 °C retained the protein repellent properties for as long as 10 days after their exposure to physiological-like conditions. The PEO-dopamine-melanin modification represents a simple and universal surface modification method for the preparation of protein repellent surfaces that could serve as a nonfouling background in various applications, such as optical biosensors and tissue engineering.
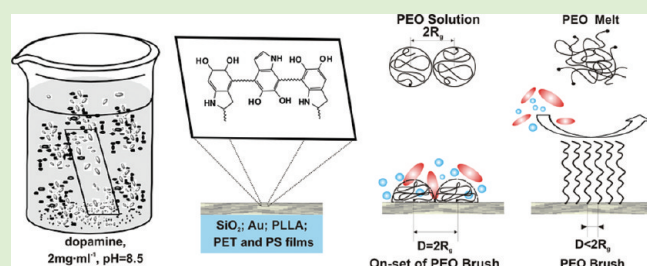
■ INTRODUCTION

The inhibition of nonspecific binding of biomacromolecules at solid—liquid interfaces is an essential issue in many fields including bioanalytical devices, drug delivery systems and biomaterials in general, because the nonspecifically bound deposits impair performance of the involved devices and materials. The inhibition of nonspecific adsorption of biomacromolecules, especially proteins, is usually accomplished by coating the fouling substrate with a suitable hydrophilic polymer.[1]

Polymer brushes represent one of the most efficient coatings that can limit the nonspecific adsorption from complex biological solutions, for example, blood plasma, below 0.2 ng·cm^{-2}, the level required for biosensing.[2,3] Being a monomolecular layer, the thickness of the polymer brush is typically in the range of 10^0-10^1 nm. Such thin and highly protein-resistant coatings are irreplaceable in certain applications, for example, in evanescent field-coupled optical biosensors.[4]

The main characteristic of polymer brushes is the stretched conformation of polymer chains along the surface normal together with parabolic density profile that results from high grafting density and interchain steric repulsion.[5] Theoretical analysis of interaction between the polymer brush and a protein based on a simplified model of polymer chains and protein molecule shows that the main factor favoring the resistance to adsorption is the osmotic repulsion. This repulsion originates in the reduction of polymer/water mixing upon brush compression with an approaching protein.[6,7] In the frame of the model, two obvious brush parameters, the grafting density σ and the degree of polymerization N, control the thermodynamics and kinetics of the protein adsorption.[7,8] A simplified outcome of the model is that the adsorption is reduced with increasing σ and N, which both contribute to the increase in the osmotic barrier.

In general, the end-tethered polymer layers may not be sufficiently dense to show the characteristics of a polymer brush.[5] Therefore, the state of the grafted layers should be assessed before declaring it a brush, for example by determining the reduced grafting density $\Sigma = \sigma \pi R_g^2$, where Σ is the ratio of the actual grafting density σ and the overlap grafting density $1/(\pi R_g^2)$ of the polymer chains with the radius of gyration R_g at specific experimental conditions of temperature and solvent.[9] The reduced grafting density equal to 1 might indicate the brush state but in the real systems this state is approached at somehow larger values because of the polydispersity of tethered chains and statistical character of grafting. Based on a literature survey of experimental data, reduced grafting densities $\Sigma > 5$ were suggested as an approximate indicator of the brush state in a good solvent.[9]

Poly(ethylene oxide) (PEO) coatings are frequently employed to inhibit nonspecific binding, especially in biomedical devices due to the low toxicity and immunogenicity of PEO.[9,10] Side-group-free constitution of PEO imparts a high mobility to the polymer chain that, together with extensive hydration,

contributes to the nonfouling efficiency of the coatings.[11] Few feasible methods are available for the preparation of PEO brushes. The surface-initiated polymerization ("grafting-from" procedure), otherwise favorite for preparation of brushes of vinylic polymers,[12] is in the case of PEO a laborious procedure.[13] Therefore, the "grafting-to" procedure with a preformed PEO bearing reactive end groups is a typical way to obtain a polymer brush. However, if the grafting is carried out from a solution in a good solvent, the grafting density rarely reaches the level indicative of the brush state because the excluded volume effect prevents the high density packing. To obtain a true PEO brush, this effect has to be either reduced or eliminated, for example, by using solvent with worse thermodynamic quality[14,15] or performing the grafting from melt.[16−18] The latter approach, less frequently utilized, has the advantage of higher achievable grafting densities, but it requires temperatures above 70 °C in order to melt PEO.

In both implementations of the "grafting-to" procedure, the result also depends on density, reactivity, and accessibility of the reactive groups on the surface. They can be introduced to the surface as reactive self-assembled monolayers (SAMs) of low-molecular-weight reagents such as functionalized alkyl-silanes,[19,20] -thiols, or -phosphates.[21] However, polymer anchoring layers, for example, from poly(glycidyl methacrylate),[22] poly(N-hydroxysuccinimidyl methacrylate),[23,24] or maleic anhydride copolymers[24] that can react with both the surface and the terminally functionalized macromolecules are much more versatile for grafting of adlayers than SAMs because they may be applied to a much wider range of materials and demonstrate higher grafting efficiency.[25]

An exceptional polymer for the preparation of anchoring layers is dopamine-melanin (also termed polydopamine). Inspired by the structure of adhesive proteins of marine mussels, Lee et al.[26] demonstrated dopamine-melanin to be a versatile functional adhesive coating. The coating was applied to flat substrates[26] and to colloidal particles.[27−30] Remarkably, unlike other polymer anchoring layers, the dopamine-melanin continuous layer can be formed in situ from an aqueous solution of dopamine by a polymerization/deposition process under mild conditions on virtually any substrate.[26]

Under alkaline conditions, the monomer, dopamine (4-(2-aminoethyl)benzene-1,2-diol), spontaneously oxidizes by dissolved oxygen. The highly reactive products formed at the end of the oxidation cascade, 5,6-dihydroxyindole, 5,6-indole-semiquinone, and -quinone,[31] eventually form a water insoluble oligomer or polymer through polycondensation,[32] presumably via 2,4′ and 2,7′ bondings between the indole units.[33,34] Dopamine-melanin oligomers self-assemble and form colloidal particles that further aggregate and form black precipitate in the solution and a thin layer on the surfaces in contact with the solution.

The mechanism underlying dopamine-melanin film formation remains unclear,[35] nevertheless, both processes (i) polymerization from the surface and (ii) adsorption of colloidal dopamine-melanin particles from solution can participate in the layer formation. The strength of dopamine-melanin binding to materials originates in the reactivity of orthoquinone/catechol subunits that may form either coordination bonds with surface metal oxides or covalent bonds with nucleophilic groups.[36,37] With the concomitant action of weaker interactions such as hydrogen bonds, van der Waals interactions, and hydrophobic interactions, the dopamine-melanin layer can firmly adhere to a wide range of materials.

In this study we evaluate the potential of dopamine-melanin coatings as a substrate independent anchoring layer for the high-density PEO grafting. A detailed investigation of dopamine-melanin growth kinetics on various materials and topography analysis of the coatings were performed using ellipsometry and AFM to gain good control over the parameters of the anchoring layer. α-Aminoethyl-ω-methoxy-poly(ethylene oxide) was covalently bound to the 5,6-indole-semiquinone and -quinone groups of dopamine-melanin. The grafting of PEO from solution and melt was compared, and the melt-grafting process was optimized. Furthermore, the stability and the resistance to protein adsorption from complex biological solutions have been tested.

■ EXPERIMENTAL SECTION

Materials. Dopamine/HCl (98.5%), human serum albumin (HSA), fibrinogen (Fbg), and human blood serum (HBS) were purchased from Sigma. Citrated human blood plasma (HBP) from single healthy donor was obtained from the Institute of Hematology and Blood Transfusion, Prague, Czech Republic. Heterobifunctional poly(ethylene oxides) α-aminoethyl-ω-methoxy-poly(ethylene oxide) (amino-PEO, M_w = 5000 g·mol^{-1}, PDI = 1.03) and α-hydroxyethyl-ω-methoxy poly(ethylene oxide) (hydroxy-PEO, M_w = 5000 g·mol^{-1}, PDI = 1.03) used in preparation of polymer brushes were purchased from Rapp Polymere (Germany). Organic solvents of analytical grade were used as received.

Substrate Preparation. One side polished silicon wafers (CZ, orientation ⟨100⟩, B-doped, resistivity 5−22 Ω cm) with ∼50 nm (OnSemiconductor, Czech Republic) and ∼260 nm (SHE-Europe Ltd.) thermal silicon dioxide (SiO$_2$) overlayer were cut into 1.2 × 2.4 cm pieces, sonicated in methanol and deionized water (Milli Q system, Millipore) for 15 min, immersed in a mixture of 25% ammonia, 30% hydrogen peroxide, and water (1:1:5 v/v/v) heated at 70 °C for 10 min, and finally, thoroughly rinsed with water. Dry samples were exposed to air plasma (25W) for 5 min just before polymer deposition. Gold-coated substrates for surface plasmon resonance (SPR) analysis and infrared spectroscopy were purchased from Litcon (Sweden) and consisted of a NBK7 glass support, ∼2 nm of titanium adhesion layer, and ∼50 nm of gold layer. They were cleaned by sonication in methanol and water for 15 min, blow dried, and exposed to air-plasma before use.

Polymer Coatings. Polyethylene terephthalate (PET), poly(L-lactide) (PLLA), and polystyrene (PS) thin films were deposited on (3-aminopropyl)triethoxysilane (APTES, Aldrich) treated silicon wafers. The silane layer was prepared from vapors for 15 min in vacuum, then heated in an oven at 120 °C for 1 h, and kept in vacuum until further use. PET (GoodFellow) was dip-coated from 12 mg·mL^{-1} solution in hexafluoroisopropanol (withdrawing speed 80 mm·min^{-1}), PS (Polymer Solutions, Inc. M_w = 154300 g·mol^{-1}, PDI = 1.68), and PLLA (synthesized by ring-opening polymerization of L-lactide,[38] M_w = 390000 g·mol^{-1}) were spin-coated from 10 mg·mL^{-1} solutions in chloroform (2000 rpm/min) to obtain 20−30 nm thick layers. The coated substrates were dried under vacuum at 120 °C for 1 h.

Dopamine-melanin Coating. Dopamine-melanin was deposited from 2 mg·mL^{-1} solution prepared by dissolution of dopamine hydrochloride in an air-saturated 10 mM Tris-HCl (pH 8.5) buffer. Based on the conclusion of Bernsmann et al.[35] and Lee et al.,[26] that the surface deposit is identical with the bulk precipitate of dopamine-melanin arising in oxygenated dopamine solution, we infer that the kinetics of the deposit formation is closely correlated with the kinetics of the bulk dopamine-melanin formation and controlled accordingly by the same reaction parameters. Therefore, the deposition of dopamine-melanin on substrates was performed in open glass dishes and under controlled stirring that provided continuous supply of oxygen through the air/solution interface. In addition, the flat substrates were kept vertical to suppress microparticle sedimentation. The coated surfaces were finally rinsed with water, sonicated in water for 15 min, and blow-dried in a stream of nitrogen.

Grafting of PEO Ad-Layer to Dopamine-melanin Layer.
α-Aminoethyl-ω-methoxy-poly(ethylene oxide) M_w = 5000 g·mol^{-1} was employed in the grafting, either from solution or from melt, to planar substrates precoated with a 10–20 nm thick dopamine-melanin layer. Grafting from solution was performed according to a procedure described by Lee et al. (5 mg·mL^{-1} of amino-PEO in 10 mM Tris buffer pH = 8.5 at 55 °C, 24 h).[26] The melt grafting was performed at 70, 90, and 110 °C in vacuum from several micrometer thick PEO layers, formed by applying 8 mg·mL^{-1} solution of amino-PEO in methanol at a surface coverage of 2 μg·mm^{-2}. The layers were first dried at 40 °C in vacuum for 1 h and only after the complete evaporation of the solvent, the temperature was elevated to the desired grafting temperatures at which the PEO is in melt state.[16–18] After 24 h of grafting, the substrates were rinsed with copious amounts of water, then immersed in water at 40 °C for 1 h under stirring to remove a noncovalently bound fraction of PEO, and finally dried in vacuum.

Stability Test. PEO/dopamine-melanin and neat dopamine-melanin layers deposited on SiO$_2$/Si and SPR chips were incubated in phosphate-buffered saline (PBS, pH = 7.4, 0.15 M phosphate, 138 mM NaCl, 2.7 mM KCl) containing 0.02 wt % sodium azide at 37 °C and kept under gentle stirring for 10 days. After the immersion periods, the substrates were rinsed with copious amounts of water and dried in vacuum before characterization.

Methods. *High Performance Liquid Chromatography (HPLC).*
HPLC analysis was performed on a low-pressure gradient LC system (Knauer, Germany) equipped with quaternary pump, automatic injection valve fitted with a 20 μL loop, column thermostat, and UV–vis Diode Array Detector (DAD). Separation in the reverse phase mode was carried out on column GraceSmart RP 18 5 μ, 250 × 4.6 mm (Grace, Deerfield, IL, U.S.A.) using isocratic elution at a flow rate of 1 mL·min^{-1} with a mobile phase (pH 2.5) of 5 mM aqueous solution of fluorobutyric acid (ion-pairing reagent) containing 10 vol % of acetonitrile. Samples of 100 μL were taken from polymerization solution in specified time intervals and diluted with 900 μL of mobile phase, which induced termination of dopamine oxidation due to a drop in pH. The monomer conversion was calculated from an integrated peak area of dopamine eluting at 3.89 min (see the Supporting Information.)

Dynamic Light Scattering (DLS). Hydrodynamic diameter of dopamine-melanin colloidal particles was measured by DLS at the scattering angle of 173° on a Zetasizer Nano-ZS, model ZEN 3600 (Malvern Instruments, U.K.), equipped with a He Ne laser λ = 632.8 nm. Freshly prepared dopamine solution at a concentration of 2 mg·mL^{-1} in an air-saturated Tris buffer (pH 8.5) was immediately filtered through a 20 nm syringe filter, 5 min thermally equilibrated, and then measured in selected times over a period of 100 min. Acquired scattering data was evaluated using DTS (Nano) software. The correlation function of micrometer-sized colloids did not show any indication of particle sedimentation such as local maxima. (See the Supporting Information.)

Atomic Force Microscopy (AFM). All images were acquired with Multimode Atomic Force Microscope NanoScope IIIa (Digital Instruments) as topological scans in tapping mode in air, using silicone probes OTESPA (Veeco Instruments) with nominal spring constant of 42 N·m^{-1} and tip radius of 7–10 nm. Areas of 10 × 10 μm^2 (512 × 512 pixels) were scanned at a rate of 1 Hz. The scans were analyzed using Gwyddion software. The dopamine-melanin grains present on the surface were identified by setting a threshold height of 15% of the maximum height value appearing in the height data. Only grains occupying areas larger than 2 × 2 pixels were taken into the analysis because smaller ones most probably arise from noise. The root-mean-square roughness value R_q of height irregularities and the autocorrelation length T were obtained from the one-dimensional autocorrelation function G_x calculated from the profiles along the fast axis

$$G_x(m) = \frac{1}{N(M-m)} \sum_{l=1}^{N} \sum_{k=1}^{M-m} z_{k+m,l} z_{k,l}$$

where $z_{i,j}$ is the height at data point with indexes i and j, M, and N are the number of points along fast and slow axis, respectively. Roughness parameters R_q and T were obtained by fitting the one-autocorrelation function with a Gaussian function

$$G_x(\tau_x) = R_q^2 \exp(-\tau_x^2/T^2)$$

where τ_x is the distance between points along the fast axis. This function describes well the autocorrelation function of randomly rough surfaces.

Transmission Electron Microscopy (TEM). Samples were prepared by floating carbon-coated TEM grids on a dopamine air/solution interface for 30 min, then rinsed with water and dried in air. TEM images were acquired with Tecnai G2 Spirit (FEI) at 120 kV acceleration voltage.

Contact Angle Measurement (CA). The static contact angles were measured with contact angle goniometer OCA 20 (Dataphysics, Germany) equipped with SCA 20 and 21 software. Drops (2 μL) were deposited on tested surfaces and their profiles were fitted with the Young–Laplace equation. Values are averages of at least three measurements recorded at different positions on each substrate.

Ellipsometry and Calculation of Grafting Density. Ellipsometry measurements were performed on Spectroscopic Imaging Auto-Nulling Ellipsometer EP^3-SE (Nanofilm Technologies GmbH, Germany) in the wavelength range of λ = 398.9–811 nm (source Xe-arc lamp, wavelength step ~10 nm) prior to and after every deposition or immersion step. To increase the measurement precision, a 10× objective and position calibrated sample stage was utilized to perform repeated measurements from the same area of 1 × 2 mm^2 on the sample and in this way to exclude the errors from the variations of the layer thicknesses throughout the substrate area. All measurements were performed at angle of incidence AOI = 70° except the measurements intended for acquiring optical constants of polymer layers (PET, PLLA, PS, PEO), which were performed at AOI = 65, 70, and 75°.

The ellipsometric data were fitted with multilayer models using EP^3-SE analysis software. The thickness and refractive indexes n of polymer layers were obtained from simultaneous fitting using Cauchy dispersion function $n = A_n + B_n/\lambda^2$ (APTES: A_n = 1.41, B_n = 6265 nm^2; PEO: A_n = 1.45, B_n = 6000 nm^2; PET: A_n = 1.58, B_n = 11500 nm^2; PLLA: A_n = 1.48, B_n = 6000 nm^2; PS: A_n = 1.59, B_n = 9155 nm^2). The Si/SiO$_2$ substrates were modeled using the dispersion functions published by Herzinger et al.[39] The gold layer was modeled as a bulk gold with a software predefined optical function because at a thickness of 50 nm and higher the layer is practically nontransparent for the light used.

The optical constants of dopamine-melanin layer, which has a broad absorption in the UV–vis region, were determined by multiple sample analysis combined with the interference enhancement method.[40] The thicknesses of dopamine-melanin films deposited on 260 nm thick SiO$_2$/Si substrates ranged from 10 to 40 nm. Ellipsometric data from these samples were acquired using UV–vis ellipsometer (J.A. Woollam Co., Inc., U.S.A.) with rotating analyzer at AOI of 65, 70, and 75° within the wavelength range of 230–1100 nm. The ellipsometric data were analyzed with WVASE-32 software using Lorentz oscillator as a dispersion model of the dielectric function of the dopamine-melanin film. In this way, unique solutions for the fitted parameters can be obtained due to significant decorrelation of the film thickness and optical constants. Obtained Lorentz parameters of the dopamine-melanin are the following: real part of high frequency dielectric constant $\varepsilon_1(\infty)$ = 1.73 ± 0.03, center energy E_n = 8.07 ± 0.30 [eV], broadening Br$_n$ = 10.01 ± 0.57 [eV], and amplitude A_n = 68.67 ± 0.19 [(eV)^2; MSE = 37]. Inclusion of a surface roughness using Bruggeman effective medium approximation (EMA)[41] to the ellipsometric model did not result in a better fit. EMA is actually valid only for values of $R_q \leq$ 10 nm and lateral dimensions $T \leq$ 10 nm.[42] The majority of our samples showed rather high lateral dimensions of $T \geq$ 150 nm and $R_q \leq$ 10 nm for which is the influence of the surface roughness on ellipsometric quantities is negligible.[43]
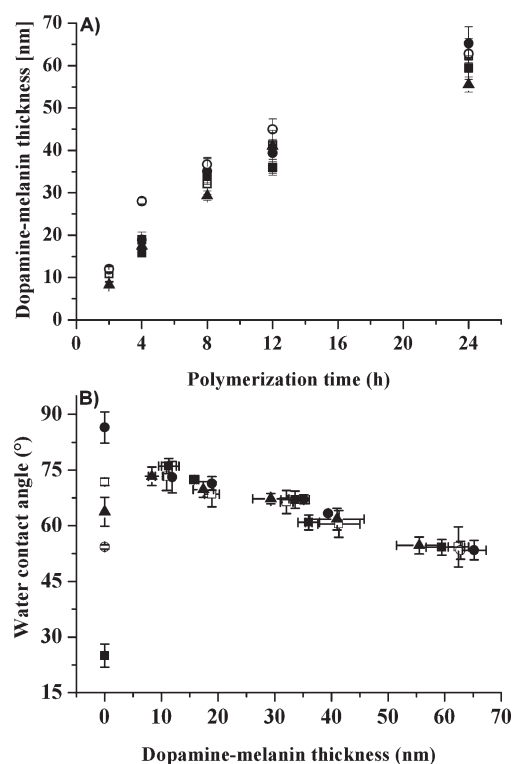
Figure 1. Ellipsometry thickness (A) and water contact angle (B) evolution of dopamine-melanin layer formed on gold (○); Si/SiO₂ (■); and PET (□), PLLA (▲), and PS (●) modified substrates. Dopamine-melanin layers were deposited on different surfaces in a single batch.

The obtained thicknesses were used to calculate the grafting density $\sigma = h\rho N_A/M_n$ and reduced grafting density $\Sigma = \sigma \pi R_g^2$, where h is the layer thickness in the dry state; $\rho = 1.09 \, \text{g/cm}^3$ is the PEO bulk density;[44] and N_A is the Avogadro constant. The radius of gyration R_g for PEO of $M_n = 5000$ in water is 3.2 nm.[45]

Reflection—Absorption Infrared Spectroscopy (RAIRS). The spectra of dry dopamine-melanin and PEO grafted to dopamine-melanin coatings on the SPR golden chips were recorded using FTIR Bruker IFS 55 spectrometer equipped with Pike Technologies 80Spec Specular reflectance accessory and polarizer (grazing angle 80°, p-polarization, MCT detector, resolution 2 cm⁻¹, 1024 scans). The spectrometer was purged continuously with dried air.

Surface Plasmon Resonance (SPR). Protein adsorption was measured with a custom-built SPR instrument (Institute of Photonics and Electronics, Academy of Sciences of the Czech Republic) utilizing the Kretschmann geometry to excite surface plasmons. The SPR chips were coated with 12 ± 0.8 nm dopamine-melanin layer and, subsequently, PEO layers were grafted. Human serum albumin (HSA; 5 mg·mL⁻¹), fibrinogen (Fbg; 1 mg·mL⁻¹) in PBS (pH 7.4), undiluted human blood serum (100% HBS), and undiluted human blood plasma (100% HBP) were flowed as analytes through the flow cell at the rate of 20 μL·min⁻¹ for 20 min. Protein—surface interactions were monitored in real time as shifts in the resonant wavelength (wavelength interrogation detection mode). The wavelength shift between two buffer baselines before and after protein injection was used to calculate the amount of irreversibly bound proteins to the surface. For the SPR sensor used in this study, a shift in the resonant frequency of 1 nm represents a surface coverage of 15 ng·cm⁻².[46] The detection limit of the SPR instrument was estimated to be the sensor response corresponding to three standard deviations of the baseline noise.[3] The average detection limit was 0.045 nm, which corresponds to 0.7 ng·cm⁻².
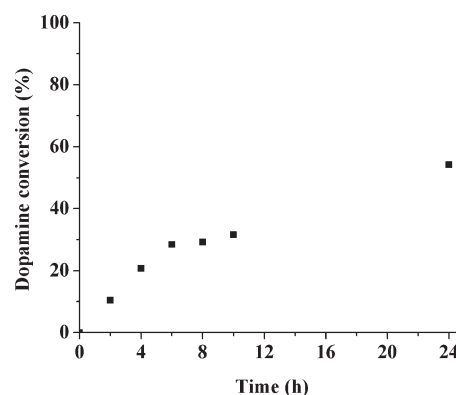

Figure 2. Conversion of dopamine by auto-oxidation in dopamine solution of 2 mg·mL⁻¹ dissolved in 10 mM Tris buffer pH 8.5 (at the beginning saturated with air) in a stirred open vessel. Dopamine was determined by HPLC.

■ RESULTS AND DISCUSSION

Optimization of Dopamine-melanin Layer Deposition. Continuous and uniform anchoring layers with reproducible reactivity and adhesion properties are essential for reproducible quality of grafted ad-layers. The first part of this study is therefore focused on the kinetics of dopamine-melanin growth and the analysis of surface properties such as topography and wettability that allow finding an optimal thickness of dopamine-melanin layer for subsequent grafting. To prepare dopamine-melanin coatings on various materials with a uniform target thickness, we followed the kinetics of dopamine-melanin film growth on a selection of materials representing important classes of materials where dopamine-melanin coating may enhance their functionality: two common polymer biomaterials, polylactide and poly(ethylene terephtalate), polystyrene as a material of cell culture dishes, gold as a common transducer surface of SPR sensors and a typical platform for self-assembled monolayers, and silicon as a reflexive supporting substrate with multiple use. Despite rather different surface energies of the materials that may influence the early stage of melanin deposition, the growth curves expressed in ellipsometric thickness (Figure 1) are very similar. The overall reaction stoichiometry suggested by Herlinger et al.[47]

$$\text{dopamine H}^+ + 2O_2 \rightarrow \text{dopaminechrome} + H^+ + 2H_2O_2$$

implies that the rate of oxygen consumption is twice higher than that of dopamine. Furthermore, considering that pH can be well controlled with buffer and that dopamine in typically employed, the reaction mixture is in large excess over oxygen (10.6 mM of dopamine ~2 g·L⁻¹ vs 0.206 mM of oxygen in oxygen-saturated solution),[26,47] it is obvious that the most critical reaction parameter controlling dopamine-melanin formation is the oxygen concentration. This was evidenced in a Quartz Crystal Microbalance experiment using a closed cell when the growth of dopamine-melanin layer reached a plateau in 30 min and, conversely, the layer continued to grow with injections of fresh reaction mixture saturated with air.[35] Therefore, the differences between the growth curves can be attributed rather to variations in oxygen supply than to the differences in materials. Moreover, the substrate surfaces coated with the melanin layers exceeding 10 nm show the same contact angles of water (Figure 1B), indicating the similarity between the films. The growth curve of dopamine-melanin on silicon within the first several hours matches quite well the data
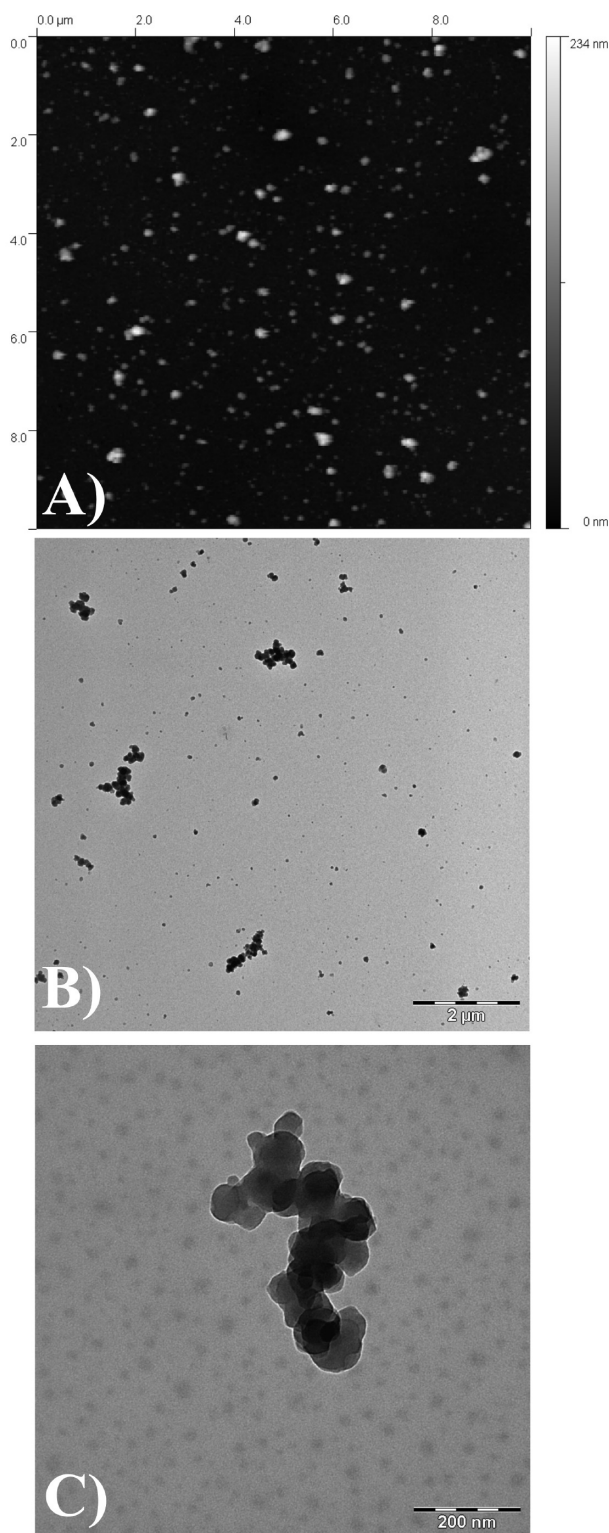
Figure 3. Representative $10 \times 10 \, \mu$m AFM scan of dopamine-melanin layer (60 nm; A). TEM images of dopamine-melanin aggregates adsorbed on carbon-coated TEM grids from the reaction mixture in 3 h (B, C).

measured by other groups with the same buffer and concentration of dopamine.[26,35,48] The small differences can be attributed again to variations in supply of oxygen and experimental techniques used to measure the film thickness. The growth of dopamine-melanin is

almost linear during the first 6 h and later it slows down[26] most probably due to the decrease in dopamine concentration. The HPLC analysis showed decrease to about 54% of the initial dopamine concentration in 24 h (Figure 2). The substantial disturbance of the dopamine-melanin formation may also originate in the oxidative action of accumulating hydrogen peroxide, which can even stop the formation of melanin if it is in excess over dopamine.[49]

Thicker anchoring layers, in the range of several tens of nanometers, may seem to be beneficial because they cover well the modified substrate. However, a detailed morphology analysis by AFM (Figure 3A) reveals the presence of 10^2-10^3 nm grains whose number and size increases with increasing time of deposition (Table 1). The corresponding roughness parameter R_q (root-mean square) increases with the increasing layer thickness and is also indicated by decreasing static contact angles (Figure 1). In addition to R_q providing an amplitude information of the surface topography, no less important parameter is the autocorrelation length T that bears a spatial information.[50] Both parameters R_q and T together fully characterize the surface topography in a statistical sense if the surface is randomly rough, which is undoubtedly the case of the dopamine-melanin layer. The surface roughness is known to affect the polarity of the reflected light, and the optical models of surface layers used to model ellipsometry data should include a correction of this effect. The detailed analysis of influence of random roughness on ellipsometric ratio implies that the effect is negligible if $R_q < 5$ nm and $T > 200$ nm.[42,43] This condition is fulfilled for dopamine-melanin layers thinner than 25 nm (Table 1). The ellipsometric data of layers with $R_q \sim 10$ nm and $T > 100$ nm should be corrected but the adequate approach based on Rayleigh-Rice theory is very complex[42] and is commonly not included in commercial ellipsometric software. Note that the effective medium approximation frequently used to include roughness into the optical model is inadequate for surfaces with stated roughness parameters.[42,43] Therefore, ellipsometry thicknesses without correction of roughness effect were compared with those obtained by the step height measurement using AFM to see the error made by omitting the roughness. The average values of both sets match very well within the error of measurement up to the thickness of 50 nm (see the Supporting Information). The calculation of thickness from uncorrected ellipsometric data is therefore justified.

The surface grains are likely adsorbed colloidal particles of dopamine-melanin that are formed in the dopamine solution from the very beginning, as evidenced by dynamic light scattering. Particles with a hydrodynamic diameter of about 100 nm appear within several minutes after dissolution of dopamine in the aerated buffer and gradually grow and reach size of micrometer during one hour (Figure 4). The intensity size distributions are unimodal up to about 30 min of polymerization, and later, a smaller fraction in the micrometer region appears (Figure 5). This new peak only indicates the presence of micrometer-sized aggregates whose concentration is much lower than that of the main peak. However, the actual course of the distribution for the size above 1 μm is distorted due to lower precision of the used instrumentation in this region. The polydispersity index of the particles expressed as a ratio of hydrodynamic radius and half-width of the peak of the intensity size distribution is between 0.2 and 0.5. A detailed structure of the adsorbed particles on surfaces was investigated by transmission electron microscopy (Figure 3B,C). The images reveal that the

Table 1. Surface Characteristics of Dopamine-melanine Layers Deposited for Different Time Periods and Subsequently Sonicated in Water[a]
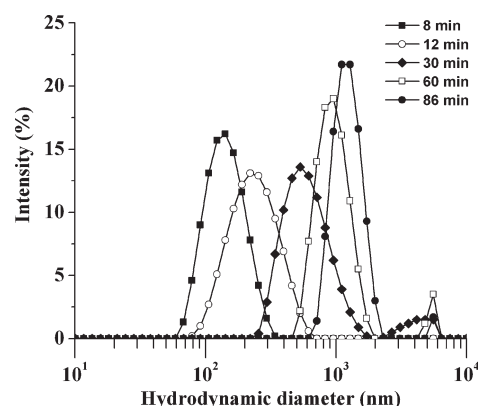
time of deposition (h)	thickness (nm)	rms roughness (nm)	autocorrelation length (nm)	density of grains (μm^{-2})	average grain height (nm)	average grain diameter (nm)
1	8 ± 1	3.0 ± 0.3	380 ± 30	1.0 ± 0.4	46 ± 29	85 ± 45
4	21 ± 1	4.0 ± 0.3	380 ± 100	1.0 ± 0.4	34 ± 11	110 ± 46
8	36 ± 9	9 ± 1	160 ± 30	3 ± 1	53 ± 14	130 ± 46
12	39 ± 4	18 ± 5	120 ± 20	3 ± 1	75 ± 23	140 ± 57
24	60 ± 3	15 ± 1	150 ± 6	3 ± 0.2	69 ± 19	140 ± 59

[a] All calculations were perfomed on 10×10 μm AFM scans. Data is given as mean value ± SD; six scans were analyzed for each layer thickness.
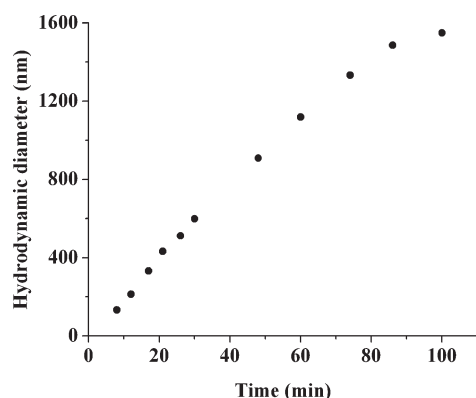
Figure 4. Growth of hydrodynamic diameter (maximum of the main peak of the intensity size distribution, Figure 5) of dopamine-melanin particles in the reaction mixture.

Figure 5. Development of the intensity size distribution of the dopamine-melanin particles in the reaction mixture containing 2 mg·mL^{-1} of dopamine in Tris buffer pH 8.5. The reaction mixture was prepared by dissolution of dopamine in the buffer followed by immediate filtration through a 20 nm (Anotop) filter. The centers of the main peaks of the distribution curves correspond to the values of hydrodynamic diameter reported in Figure 4.

particles detected by AFM (Figure 3A) are aggregates of smaller spherical nanoparticles with the diameter between 30 and 100 nm. A similar structural organization was found in natural eumelanin from cuttlefish *Sepia officinalis*, where the micrometer pigment grains are composed of aggregates of particles with diameters of 100−200 nm.[51] The adsorbed dopamine-melanin nanoparticle aggregates are a potential source of defects in grafted ad-layers. Despite simple precautions that reduce the number of adsorbed aggregates such as vertical orientation of substrates in dopamine solution and application of ultrasound as a finishing step, the thinner layers up to 20 nm retain rms roughness of several nanometers and contain surface grains 30−50 nm high, with a surface concentration of several grains per μm^2.
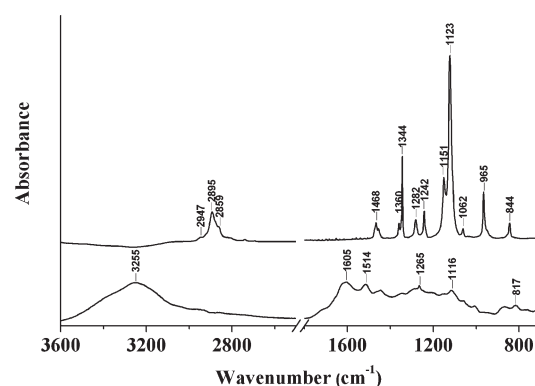
The target thickness of dopamine-melanin anchoring layers should be on the one hand as thin as possible to limit the number of surface grains and corresponding surface roughness. On the other hand, they should be thick enough to form a confluent, hole-free layer. The lower boundary of the thickness range can be guessed from the cyclic voltametry data by Bernsmann et al.[35,52] that reported impermeability of the dopamine-melanin layers for ferrocyanide anions if the thickness exceeded 5 nm. Overall, based on the mentioned results, an optimal thickness range of the dopamine-melanin layer intended as an anchoring layer seems to be between 10 and 20 nm. The film growth is a fairly reproducible process regardless of the modified material if the supply of oxygen and other reaction conditions are kept constant. For further experiments in this study, the dopamine-melanin thickness specified above was applied.

Grafting of Amino-PEO to Dopamine-melanin. Grafting from melt of amino-terminated methoxy-poly(ethylene oxide) (M_w = 5000 g·mol^{-1}) to dopamine-melanin layer was performed at a temperature of 110 °C, but also at milder temperatures of 90 and 70 °C, closer to the melting point of PEO, which would be more convenient in practical applications. Moreover, the grafting was carried out in vacuum to prevent oxidative degradation of PEO. As a reference, we performed grafting from solution following the procedure published by Lee et al.,[26] where the PEO ad-layers on dopamine-melanin were prepared by grafting of amino-PEO (M_w = 5000 g·mol^{-1}) from 10 mM Tris buffer (pH 8.5) at 50 °C and their biofouling-resistant properties were demonstrated in a protein adsorption assay. The dopamine-melanin anchoring layer was 12 nm thick for both grafting procedures. Additionally, reference thermal treatments on neat dopamine-melanin layers were performed under the same conditions as in the case of PEO grafting. It is noteworthy that the exposure to higher temperature did not alter the anchor layer characteristics (see Supporting Information, Figures S9 and S10). In Table 2 the thicknesses and other characteristics of the grafted layers are listed. The chain densities of the layers grafted from melt increase with increasing grafting temperature as a result of higher chain mobility. Not surprisingly, grafting densities of layers from melt are much higher than of those prepared from solution. They are also several times higher than

Table 2. Characteristics of Amino-PEO Layers Grafted to Dopamine-melanin

environment of grafting	grafting temperature (°C)	thickness (nm)	chain density (nm^{-2})	reduced chain density in H$_2$O	contact angle (°)
solution	50	1.7 ± 0.2	0.22	7.2	49 ± 1
melt	70	5.1 ± 0.3	0.67	21.6	17 ± 1
melt	90	8.9 ± 0.5	1.17	37.6	15 ± 1
melt	110	13.9 ± 0.4	1.83	58.7	12 ± 1
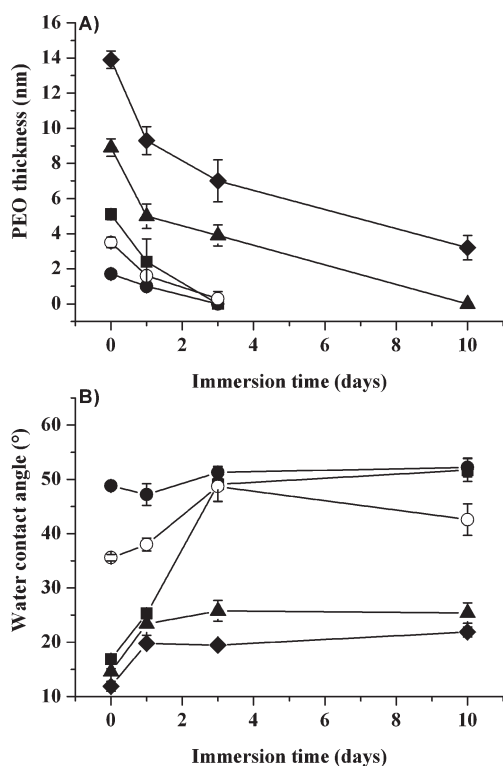
Figure 6. Ellipsometric PEO thickness (A) and contact angle evolution (B) vs time of immersion of PEO/dopamine-melanin coating in PBS (37 °C, pH = 7.4) (mean value ± SD, n = 3). Amino-PEO was grafted from solution at 55 °C (●) and from melt at 70 °C (■), 90 °C (▲) and 110 °C (♦); the nonreactive hydroxy-PEO (○) was applied from melt at 110 °C. The time of grafting common for all conditions was 24 h.

Figure 7. RAIRS spectra of the neat dopamine-melanin (lower curve) and amino-PEO (upper curve) thin layers.

A covalent binding of alkylamines to dopamine-melanin has been experimentally well supported in the literature[36] and we assume it is effective also for amino-PEO. In addition to the covalent bonds, noncovalent interactions may also participate in the adhesion of PEO to dopamine-melanin. To assess the noncovalent contribution we used a hydroxy-PEO as a nonreactive surrogate of the amino derivative in the melt grafting procedure at 110 °C. After grafting and a 1 h washing step in 40 °C warm water under stirring, surprisingly a PEO layer 3.5 ± 0.3 nm thick exhibiting contact angle of 37° was found. Compared to monolayers of PEO-diol (M_w = 3400) physisorbed from aqueous solution to bare[57] or methylated silica,[58] it is 1 order of magnitude thicker. Such a thick PEO layer is likely formed as a result of multiple surface-monomer unit interactions facilitated by the contact of the PEO melt with the anchoring layer. This finding suggests that the layers of amino-terminated PEO grafted from melt can contain a significant fraction of only physisorbed PEO. This fraction may be liable to release during a long-time exposure to an aqueous solution or to another good solvent.

Stability of PEO Layers. The stability of PEO coatings is crucial for their performance, and its deterioration could affect nonspecific binding of biomacromolecules and decrease surface concentration of free end-groups that are essential in some applications for immobilization of ligands. The stability test was performed by exposing the PEO/dopamine-melanin and the neat dopamine-melanin layers on silicon wafers to PBS buffer for a period of 10 days. In days 1, 3, and 10, the changes of ellipsometric thickness together with contact angles of the dried samples were recorded (Figure 6 and Supporting Information, Figure S11). In a parallel experiment, the stability of the PEO layer grafted at 110 °C and neat dopamine-melanin was followed with RAIRS in a grazing incidence mode, which provided deeper inside into the changes of the PEO/dopamine-melanin double layer and allowed to separately follow both components. For this experiment the layers were prepared on gold-coated glass slides and treated just as that on silicon.

densities of similar PEO layers prepared under cloud point conditions reported in literature,[53,54] whose density for the same molecular weight of PEO does not exceed 0.4 nm^{-2}. Nevertheless, all grafted layers, including that one prepared from solution, meet the reduced grafting density criterion (Σ > 5) for the brush state. The differences between brushes prepared under different conditions are indicated by contact angle measurements. While the thinnest brush close to the mushroom-brush conformational transition shows a contact angle of 49°, the three and more times thicker layers are much more wettable with contact angles of 12−17°. Such low contact angles are somehow contradictory to the 30−40° often reported in the literature for PEO layers.[18,55] However, more examples of PEO brushes with comparable grafting densities and molecular weight of PEO chains exist that also exhibit contact angles below 30°.[16,56] We believe that the contact angles not only reflect the grafting density and molecular weight of PEO chains, but also the morphology and chemical structure of the underlying substrate.
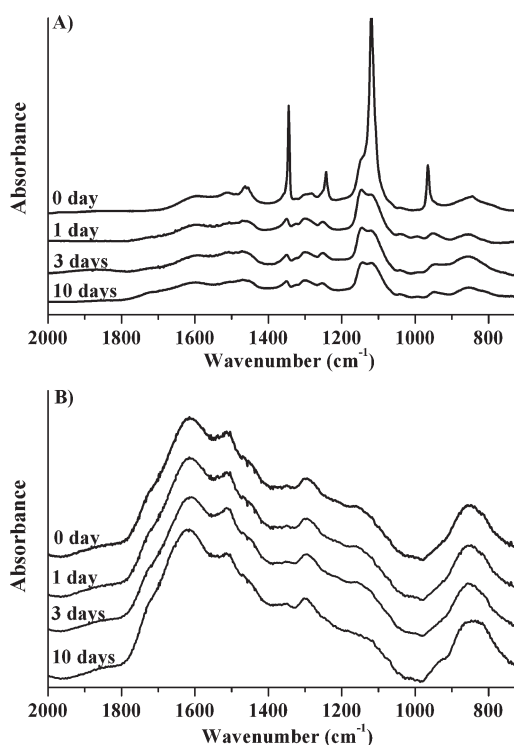
Figure 8. Evolution of RAIRS spectra of PEO/dopamine-melanin formed from melt at 110 °C (A) and bare dopamine-melanin (B) upon immersion in PBS at 37 °C.

The infrared spectra of the neat components are shown in Figure 7. The spectrum of dopamine-melanin has a broad band diffusion character with poorly resolved bands in the region down from 1800 cm^{-1} indicating many overlapping vibration modes. Generally, the spectrum reflects the highly complex structure of dopamine-melanin.[59,60] The film of neat amino-PEO deposited directly on gold shows pronounced sharp and narrow bands whose assignment was comprehensively described in the literature.[61,62] The spectrum of PEO/dopamine-melanin double layer in Figure 8A (top spectrum) shows bands of both components. The bands of PEO slightly widened, the maximum of its most prominent band in the 1100 cm^{-1} region shifted from 1123 to 1119 cm^{-1} and the sideband 1151 cm^{-1} became poorly resolved. This spectral region is mainly due to deformational ($-CH_2-$) and stretching skeletal ($-C-O-C-$) vibrations and it is known to be sensitive to several factors, namely, crystallinity and conformational states of PEO.[62] The PEO/dopamine-melanin double layer prepared from melt at 110 °C was immersed in PBS for 1−10 days, shortly rinsed with water, dried, and RAIRS spectra were measured in an exact time interval. As it is seen in Figure 8A, all PEO bands became broader and a sharp drop of intensity of the band 1119 cm^{-1} was observed. Such changes are typical for the transfer of PEO from the solid to liquid state characterized by the loss of crystallinity and a decreased contribution of the *trans*-conformation.[62] More-over, the integral intensity of all PEO bands partly decreased with the time of immersion indicating dissolution of PEG, mainly during the first day of immersion. The residual content of PEO after ten days of immersion in PBS can be estimated to 42%. On the other hand, the bands of dopamine-melanin in the region 1800−1500 cm^{-1} remained essentially unchanged during the immersion indicating the stability of the dopamine-melanin layer.

The neat dopamine-melanin layer immersed in PBS (Figure 8B) showed only a small decrease in the broad absorption band in the region of 1480−920 cm^{-1} and an increase in absorption at about 840 cm^{-1}, which indicates structural or morphological changes of the layer, probably due to the increased degree of hydration. Thus, the primarily released component was PEO.

More extended and quantitative data on release of PEO were collected from ellipsometric measurements shown in Figure 6A. The optical model used for calculation of PEO thickness included the constant thickness of the dopamine-melanin layer as determined before the grafting. The optical model complies with the observation of stable neat dopamine-melanin films upon the immersion in PBS (Figure 8B and Supporting Information, Figure S11). All the PEO layers examined in the study, regardless of the grafting conditions, showed a gradual decrease in thickness without leveling off during the 10 days of the experiment. The half-life of layers grafted from melt was between 2 and 3 days and those grafted from solution was only about 1 day. Moreover, the thinner layers prepared by the grafting from solution or grafting from melt at 70 °C released PEO almost completely during 10 days. These observations are in accordance with water CA changes that in general increase with decreasing thickness of PEO layer as the less wettable dopamine-melanin surface is revealed (Figure 6B). In the case of PEO layers formed at 90 °C even after 10 days of immersion we observe rather low CA values although ellipsometric data show almost negligible thickness of these layers. Despite the precautions of performing the measure-ments from the same area on the sample, errors arising from variations of the thickness of the anchor layer cannot be completely avoided. The measured low CA values indicate that the actual thickness of the PEO layers in this case might be underestimated.

In the previous section, we pointed out that the grafted layers of amino-PEO may contain a certain fraction of PEO bound only by physical adsorption. If only this fraction dissolves during incubation with PBS, the thickness of the PEO layer should reach a plateau corresponding to the remaining covalently bound fraction. The observed continuing decay, however, may imply that also the covalently bound fraction of PEO is released. We suggest three possible mechanisms of release of covalently bound PEO that can all simultaneously participate in the process: (i) hydrolytical cleavage of the anchor bond between PEO and dopamine-melanin, for example, Schiff-base between aliphatic amine and *ortho*-quinone,[63] (ii) dissolution of colloidal assem-blies composed of PEO shell and dopamine-melanin oligomer core, (iii) oxidative degradation of PEO chains.

To assess the significance of the first mechanism, the PEO-dopamine-melanin layers and the neat dopamine-melanin layers were exposed to 132 mM solution of sodium borohydride in methanol for 1 h to reduce the Schiff-base bonds to stable secondary amines prior to the stability test in PBS. The PEO grafted layers treated with borohydride degraded even faster as compared to untreated layers (Supporting Information, Figure S12). Moreover, the action of borohydride also slightly destabi-lized the neat dopamine-melanin layer in PBS. Obviously, regardless of the stabilization of the possibly formed Schiff-adduct, the reducing agent disturbs the catechol-quinone bond-ing contributing to formation of the supramolecular structure of dopamine-melanin.

The second degradation mechanism originates in the oligomeric nature of the dopamine-melanin. The surface of the dopamine-melanin grafted with PEO thus has to contain dopamine-melanin

Table 3. Nonspecific Protein Adsorption on PEO/Dopamine-melanin Layers as Determined by SPR (mean value $\pm$ SD, $n = 3$)[a]

surface, grafting conditions (immersion time in PBS)	PEO thickness (nm)	PEO grafting density (nm^{-2})	PEO reduced chain density in water	HSA	Fbg	HBP	HBS
				Adsorbed Mass (ng·cm^{-2})			
bare gold				110 ± 54	320 ± 110	302 ± 74	500 ± 50
amino-PEO, solution	1.3 ± 0.7	0.16	5.3	68 ± 2	200 ± 3	300 ± 3	140 ± 8
amino-PEO, melt, 70 °C	5.6 ± 1.6	0.71	23	0	0	5 ± 1	35 ± 8
amino-PEO, melt, 90 °C	7.8 ± 1.1	0.99	32	0	0	6 ± 1	24 ± 5
amino-PEO, melt, 110 °C	11.0 ± 1.5	1.39	45	0	0	2 ± 1	14 ± 2
Amino-PEO Layer Grafted from Melt at 110 °C after Exposure to PBS							
1 day	6.5 ± 0.8	0.82	28			90 ± 40	23 ± 10
10 days	5.3 ± 0.9	0.67	22			90 ± 10	27 ± 3

[a] Values 0 mean that the adsorption was bellow the detection limit of the instrument (0.7 ng·cm^{-2}). Solutions: 100% human blood plasma (HBP), 100% human blood serum (HBS); 5 mg·mL^{-1} human serum albumin (HSA), 1 mg·mL^{-1} fibrinogen (Fbg). All solutions were prepared from PBS (pH = 7.4).

oligomers with several PEO chains bound that under swelling in water can pull the oligomer into the solution. Although there is no clear support for such a mechanism in the expected concomitant decrease of dopamine-melanin infrared bands, taking into account the weight fraction of a single dopamine-melanin oligomer (M_w 500—1500 g·mol^{-1})[64] in the supposedly released particles containing several PEO chains of molecular weight of 5000, this mechanism cannot be excluded.

The degradation of PEO layers through oxidative scission of the PEO was identified under similar conditions in self-assembled monolayers of PEO copolymers on titanium oxide.[65] The reported decrease of the PEO thickness was 60% after 7 days in 160 mM HEPES buffer in the dark, but it appeared to be controlled by pH and ionic strength of the solution. Other studies, where the PEO chains were bound to the surface through a silane layer and where the layer degradation can proceed only through hydrolysis of the anchor bond and oxidative degradation, reported a thickness decrease no more than 16% in two weeks.[21,66] Therefore, the oxidative degradation can also be a plausible degradation mode of the PEO grafted layer.

Resistance to Protein Adsorption. The practical utility of PEO coatings is based on both the efficiency to reduce protein adsorption and the ability to maintain this function. To examine performance of the PEO-dopamine-melanin coatings under a wider range of conditions occurring in diverse applications, we measured protein adsorption from single-protein solutions of HSA (5 mg·mL^{-1}) and fibrinogen (1 mg·mL^{-1}) as well as from undiluted blood plasma and blood serum. The experiments were performed using a SPR technique with a detection limit of 0.7 ng·cm^{-2}. The amount of adsorbed proteins at PEO layers with different grafting densities is shown in Table 3. The brushes grafted from solution following the procedure of Lee et al.[26] showed only a minor reduction of the fouling from single protein solutions and complex media compared to the bare gold. A considerable improvement was observed with brushes prepared from melt showing more than four times higher grafting densities. The PEO brushes prepared from melt suppressed the fouling from single protein solutions below the detection limit and to amounts of 2 ± 1 ng·cm^{-2} and 14 ± 2 ng·cm^{-2} from blood plasma and serum, respectively, amounts typically reported for different polymer brushes grown by surface initiated atom radical polymerization (ATRP).[67−69] However, if zwitterionic brushes are grown by surface-initiated ATRP from SAM surface formed on gold, the nonspecific protein adsorption from

complex body fluids can be reduced to 0.2 ng·cm^{-2}, like in the case of 15—20 nm thick poly(carboxybetaine acrylamide) and poly(carboxybetaine methacrylate) brushes.[2,3,70]

After incubation of PEO brushes prepared from melt at 100 °C in PBS (37 °C, pH = 7.4) for up to 10 days we have observed an increase in nonspecific protein adsorption due to the decrease of PEO grafting density (Table 3). With decreasing PEO density, the adsorption of proteins may be also enhanced by disclosing the negative charge on the dopamine-melanin layers[71] which results in 90 ng·cm^{-2} of adsorbed proteins from blood plasma. However, during the 10 days of immersion the adsorption from blood serum remained below 30 ng·cm^{-2}, amounts reported for poly(hydroxy-oligoethylene glycol methacrylate) and poly-(methoxy-oligoethylene glycol methacrylate) brushes.[72,73] Nevertheless, our modification route suppresses protein adsorption to levels that are low enough to block cell adhesion. The PEO layers grafted from melt at 110 °C to dopamine-melanin anchor layer are therefore excellent protein adsorption resistant coatings able to protect any material surface from biofouling or if enhanced with cell adhesion ligands they can serve as biospecific coatings for biomaterial surfaces or cell cultivation studies.

■ CONCLUSION

We demonstrated that the dopamine-melanin growth kinetics and the resulting layer are independent of the substrate. The oxygen concentration appears to be the critical controlling parameter for the film growth under typically used deposition conditions. Furthermore, the adsorption of dopamine-melanin colloidal particles from solution occurs during the layer growth, which is manifested in increasing surface roughness with increasing layer thickness. The surface inhomogeneities from the adsorbed nanoparticles may be the source of defects in the adlayers and therefore we suggested an optimal thickness of the dopamine-melanin layer between 10 and 20 nm. The dopamine-melanin coatings are suitable anchoring layers for grafting of amino-PEO from melt providing polymer brushes with a more than three times higher chain density than the layers grafted from polymer solution. These grafted layers are highly resistant to protein adsorption from whole blood serum and plasma and exhibit adsorption levels typical for polymer brushes formed by "grafting from" approach. However, they also decompose during several days immersion in PBS, partly due to the release of physisorbed PEO, but also by other mechanisms that are not

clear and will be a subject of further studies. Despite the partial PEO release, the coatings retain sufficiently high resistance to protein adsorption from complex biological media up to 10 days of immersion in PBS. The proposed PEO-dopamine-melanin modification represents a simple and universal surface modification method for the creation of protein-resistant surfaces suitable for demanding applications like optical biosensors and tissue engineering.

■ ASSOCIATED CONTENT

ⓢ Supporting Information. Determination of dopamine-melanin optical dispersion function by ellipsometry using multiple sample analysis combined with interference enhancement method, representative AFM images of height profiles of dopamine-melanin layers, comparison of dopamine-melanin film thickness obtained by AFM and ellipsometry, dynamic light scattering second order autocorrelation function of dopamine-melanin colloidal solution, effects of thermal treatment on dopamine-melanin ellipsometric and RAIRS spectra, changes of dopamine-melanin ellipsometric film thickness and water CA under immersion conditions, and stability of PEO on dopamine-melanin and neat dopamine-melanin films upon exposure to reducing agent are shown. This material is available free of charge via the Internet at http://pubs.acs.org.

■ AUTHOR INFORMATION

Corresponding Author
*Tel.: +420-296809225. Fax: +420-296809410. E-mail: georgievski@imc.cas.cz.

■ ACKNOWLEDGMENT

■ REFERENCES

(1) Nath, N.; Hyun, J.; Ma, H.; Chilkoti, A. *Surf. Sci.* **2004**, *570*, 98–110.

(2) Vaisocherova, H.; Yang, W.; Zhang, Z.; Cao, Z.; Cheng, G.; Piliarik, M.; Homola, J.; Jiang, S. *Anal. Chem.* **2008**, *80*, 7894–7901.

(3) Rodriguez Emmenegger, C.; Brynda, E.; Riedel, T.; Sedlakova, Z.; Houska, M.; Alles, A. B. *Langmuir* **2009**, *25*, 6328–6333.

(4) Homola, J. *Chem. Rev.* **2008**, *108*, 462–493.

(5) Milner, S. T.; Witten, T. A.; Cates, M. E. *Macromolecules* **1988**, *21*, 2610–2619.

(6) Leckband, D.; Sheth, S.; Halperin, A. *J. Biomater. Sci., Polym. Ed.* **1999**, *10*, 1125–1147.

(7) Halperin, A. *Langmuir* **1999**, *15*, 2525–2533.

(8) Jeon, S. I.; Lee, J. H.; Andrade, J. D.; de Gennes, P. G. *J. Colloid Interface Sci.* **1991**, *142*, 149–158.

(9) Brittain, W. J.; Minko, S. *J. Polym. Sci., Part A: Polym. Chem.* **2007**, *45*, 3505–3512.

(10) Frank, B.; Gast, A. P.; Russell, T. P.; Brown, H. R.; Hawker, C. *Macromolecules* **1996**, *29*, 6531–6534.

(11) Lee, J. H.; Lee, H. B.; Andrade, J. D. *Prog. Polym. Sci.* **1995**, *20*, 1043–1079.

(12) Barbey, R.; Lavanant, L.; Paripovic, D.; Schüwer, N.; Sugnaux, C.; Tugulu, S.; Klok, H.-A. *Chem. Rev.* **2009**, *109*, 5437–5527.

(13) Quirk, R. P.; Mathers, R. T.; Cregger, T.; Foster, M. D. *Macromolecules* **2002**, *35*, 9964–9974.

(14) Unsworth, L. D.; Tun, Z.; Sheardown, H.; Brash, J. L. *J. Colloid Interface Sci.* **2005**, *281*, 112–121.

(15) Huang, H.; Penn, L. S. *Macromolecules* **2005**, *38*, 4837–4843.

(16) Zdyrko, B.; Varshney, S. K.; Luzinov, I. *Langmuir* **2004**, *20*, 6727–6735.

(17) Zdyrko, B.; Klep, V.; Luzinov, I. *Langmuir* **2003**, *19*, 10179–10187.

(18) Roosjen, A.; Kaper, H. J.; van der Mei, H. C.; Norde, W.; Busscher, H. J. *Microbiology* **2003**, *149*, 3239–3246.

(19) Michaud, G. A.; Snyder, M. *BioTechniques* **2002**, *33*, 1308–1316.

(20) Luzinov, I.; Julthongpiput, D.; Malz, H.; Pionteck, J.; Tsukruk, V. V. *Macromolecules* **2000**, *33*, 1043–1048.

(21) Ulman, A. *Chem. Rev.* **1996**, *96*, 1533–1554.

(22) Zdyrko, B.; Iyer, K. S.; Luzinov, I. *Polymer* **2006**, *47*, 272–279.

(23) Feng, C. L.; Zhang, Z. Z.; Forch, R.; Knoll, W.; Vancso, G. J.; Schonherr, H. *Biomacromolecules* **2005**, *6*, 3243–3251.

(24) Pompe, T.; Zschoche, S.; Herold, N.; Salchert, K.; Gouzy, M. F.; Sperling, C.; Werner, C. *Biomacromolecules* **2003**, *4*, 1072–1079.

(25) Iyer, K. S.; Zdyrko, B.; Malz, H.; Pionteck, J.; Luzinov, I. *Macromolecules* **2003**, *36*, 6519–6526.

(26) Lee, H.; Dellatore, S. M.; Miller, W. M.; Messersmith, P. B. *Science* **2007**, *318*, 426–430.

(27) Fei, B.; Qian, B. T.; Yang, Z. Y.; Wang, R. H.; Liu, W. C.; Mak, C. L.; Xin, J. H. *Carbon* **2008**, *46*, 1795–1797.

(28) Gao, J. H.; Gu, H. W.; Xu, B. *Acc. Chem. Res.* **2009**, *42*, 1097–1107.

(29) Lee, Y. H.; Lee, H.; Kim, Y. B.; Kim, J. Y.; Hyeon, T.; Park, H.; Messersmith, P. B.; Park, T. G. *Adv. Mater. (Weinheim, Ger.)* **2008**, *20*, 4154–4157.

(30) Zhang, M.; Zhang, X. H.; He, X. W.; Chen, L. X.; Zhang, Y. K. *Chem. Lett.* **2010**, *39*, 552–553.

(31) Chang, J. C.; Hsu, S.; Chen, D. C. *Biomaterials* **2009**, *30*, 6265–6275.

(32) Bu'Lock, J. D.; Harley-Mason, J. *J. Chem. Soc.* **1951**, 703.

(33) d'Ischia, M.; Napolitano, A.; Pezzella, A.; Meredith, P.; Sarna, T. *Angew. Chem., Int. Ed.* **2009**, *48*, 3914–3921.

(34) Panzella, L.; Pezzella, A.; Napolitano, A.; d'Ischia, M. *Org. Lett.* **2007**, *9*, 1411–1414.

(35) Bernsmann, F.; Ponche, A.; Ringwald, C.; Hemmerle, J.; Raya, J.; Bechinger, B.; Voegel, J. C.; Schaaf, P.; Ball, V. *J. Phys. Chem. C* **2009**, *113*, 8234–8242.

(36) Lee, H.; Scherer, N. F.; Messersmith, P. B. *Proc. Natl. Acad. Sci. U.S.A.* **2006**, *103*, 12999–13003.

(37) Land, E. J.; Ramsden, C. A.; Riley, P. A. In *Quinones and Quinone Enzymes*, Part A; Sies, H., Packer, L., Eds.; Academic Press, Inc.: San Diego, CA, 2004; Vol. 378, pp 88−109.

(38) Leenslag, J. W.; Pennings, A. J. *Makromol. Chem.* **1987**, *188*, 1809–1814.

(39) Herzinger, C. M.; Johs, B.; McGahan, W. A.; Woollam, J. A.; Paulson, W. *J. Appl. Phys.* **1998**, *83*, 3323–3336.

(40) McGahan, W. A.; Johs, B.; Woollam, J. A. *Thin Solid Films* **1993**, *234*, 443–446.

(41) Aspnes, D. E.; Theeten, J. B. *Phys. Rev. B* **1979**, *20*, 3292–3302.

(42) Franta, D.; Ohlidal, I. *J. Opt. A: Pure Appl. Opt.* **2006**, *8*, 763–774.

(43) Franta, D.; Ohlidal, I. *Opt. Commun.* **2005**, *248*, 459–467.

(44) *Handbook of Fine Chemicals and Laboratory Equipment*; Aldrich: Milwaukee, WI, 2003−2004; p 1515.

(45) Stuart, M. A. C.; Waajen, F.; Cosgrove, T.; Vincent, B.; Crowley, T. L. *Macromolecules* **1984**, *17*, 1825–1830.

(46) Gao, C.; Li, G.; Xue, H.; Yang, W.; Zhang, F.; Jiang, S. *Biomaterials* **2010**, *31*, 1486–1492.

(47) Herlinger, E.; Jameson, R. F.; Linert, W. *J. Chem. Soc., Perkin Trans. 2* **1995**, 259–263.

(48) Postma, A.; Yan, Y.; Wang, Y. J.; Zelikin, A. N.; Tjipto, E.; Caruso, F. *Chem. Mater.* **2009**, *21*, 3042–3044.

(49) Swan, G. A.; Wright, D. *J. Chem. Soc.* **1954**, 381–384.

(50) Hoganson, D. M.; Pryor, H. I.; Spool, I. D.; Burns, O. H.; Gilmore, J. R.; Vacanti, J. P. *Tissue Eng., Part A* **2010**, *16*, 1469–1477.

(51) Clancy, C. M. R.; Simon, J. D. *Biochemistry* **2001**, *40*, 13353–13360.

(52) Bernsmann, F.; Frisch, B.; Ringwald, C.; Ball, V. *J. Colloid Interface Sci.* **2010**, *344*, 54–60.

(53) Unsworth, L. D.; Sheardown, H.; Brash, J. L. *Langmuir* **2005**, *21*, 1036–1041.

(54) Hamilton-Brown, P.; Gengenbach, T.; Griesser, H. J.; Meagher, L. *Langmuir* **2009**, *25*, 9149–9156.

(55) Stuart, M. A. C.; de Vos, W. M.; Leermakers, F. A. M. *Langmuir* **2006**, *22*, 1722–1728.

(56) Piehler, J.; Brecht, A.; Valiokas, R.; Liedberg, B.; Gauglitz, G. *Biosens. Bioelectron.* **2000**, *15*, 473–481.

(57) Muller, D.; Malmsten, M.; Tanodekaew, S.; Booth, C. *J. Colloid Interface Sci.* **2000**, *228*, 317–325.

(58) Muller, D.; Malmsten, M.; Tanodekaew, S.; Booth, C. *J. Colloid Interface Sci.* **2000**, *228*, 326–334.

(59) Ju, K. Y.; Lee, Y.; Lee, S.; Park, S. B.; Lee, J. K. *Biomacromolecules* **2011**, *12*, 625–632.

(60) Bilinska, B. *Spectrochim. Acta, Part A* **2001**, *57*, 2525–2533.

(61) Matsuura, H.; Miyazawa, T. *Bull. Chem. Soc. Jpn.* **1968**, *41*, 1798–1808.

(62) Rozenberg, M.; Loewenschuss, A.; Marcus, Y. *Spectrochim. Acta, Part A* **1998**, *54*, 1819–1826.

(63) Grünanger, P. In *Methoden der Organischen Chemie (Houben-Weyl)*, 4th ed.; Müller, E., Bayer, O., Grundmann, C., Eds.; Georg Thieme Verlag: Stuttgart, 1979; Vol. VII/3b, p 236.

(64) Napolitano, A.; Pezzella, A.; Prota, G.; Seraglia, R.; Traldi, P. *Rapid Commun. Mass Spectrom.* **1996**, *10*, 468–472.

(65) Zoulalian, V.; Zurcher, S.; Tosatti, S.; Textor, M.; Monge, S.; Robin, J.-J. *Langmuir* **2010**, *26*, 74–82.

(66) Hilderbrand, S. A.; Weissleder, R. *Curr. Opin. Chem. Biol.* **2010**, *14*, 71–79.

(67) Gao, C. L.; Li, G. Z.; Xue, H.; Yang, W.; Zhang, F. B.; Jiang, S. Y. *Biomaterials* **2010**, *31*, 1486–1492.

(68) Li, G. Z.; Xue, H.; Cheng, G.; Chen, S. F.; Zhang, F. B.; Jiang, S. Y. *J. Phys. Chem. B* **2008**, *112*, 15269–15274.

(69) Rodriguez-Emmenegger, C.; Kylian, O.; Houska, M.; Brynda, E.; Artemenko, A.; Kousal, J.; Alles, A. B.; Biederman, H. *Biomacromolecules* **2011**, *12*, 1058–1066.

(70) Vaisocherová, H.; Zhang, Z.; Yang, W.; Cao, Z.; Cheng, G.; Taylor, A. D.; Piliarik, M.; Homola, J.; Jiang, S. *Biosens. Bioelectron.* **2009**, *24*, 1924–1930.

(71) Ball, V. *Colloids Surf., A* **2010**, *363*, 92–97.

(72) Hucknall, A.; Rangarajan, S.; Chilkoti, A. *Adv. Mater. (Weinheim, Ger.)* **2009**, *21*, 2441–2446.

(73) Gautrot, J. E.; Trappmann, B.; Oceguera-Yanez, F.; Connelly, J.; He, X.; Watt, F. M.; Huck, W. T. S. *Biomaterials* **2010**, *31*, 5030–5041.